

Assembly of New Coordination Frameworks in a pH-Controlled Medium: Syntheses, Structures, and Properties of $\frac{3}{\infty}[\text{Cd}(\text{Hpdc})(\text{H}_2\text{O})]$ and $\frac{3}{\infty}[\text{Cd}_3(\text{pdc})_2(\text{H}_2\text{O})_2]$

Long Pan, Xiaoying Huang, and Jing Li¹

Department of Chemistry, Rutgers University, Camden, New Jersey 08102

Two 3D cadmium coordination networks $\frac{3}{\infty}[\text{Cd}(\text{Hpdc})(\text{H}_2\text{O})]$ (1) and $\frac{3}{\infty}[\text{Cd}_3(\text{pdc})_2(\text{H}_2\text{O})_2]$ (2) have been synthesized from hydrothermal solutions at 150°C. Single-phased samples of both compounds can be isolated by adjusting the acidity level of the reactions. Both structures are constructed by a single, multifunctional ligand, 3,5-pyrazoledicarboxylic acid (H_3pdc), in different coordination modes. Both 1 and 2 crystallize in the monoclinic crystal system, space group $P2_1/c$ (No. 14) with $a = 6.436(1)$ Å, $b = 12.283(2)$ Å, $c = 8.934(2)$ Å, $\beta = 104.23(3)^\circ$, $Z = 4$ for 1, and $a = 9.744(2)$ Å, $b = 9.821(2)$ Å, $c = 7.496(1)$ Å, $Z = 2$ for 2. Both compounds represent new structure types. All metal atoms are seven-fold coordinated in 1 and six-fold coordinated in 2. A comparison is made between the title compounds and related lanthanide series on the coordination habit of the metals and the ligand, as well as the effect of pH on the final products. TGA studies indicate that loss of coordinated water molecules in 1 and 2 occurs at around 213 and 179°C, respectively, and the decomposition process completes at about 620 and 480°C for 1 and 2, respectively. © 2000 Academic Press

Key Words: coordination polymers; cadmium compounds; 3,5-pyrazodicarboxylic acid; hydrothermal synthesis.

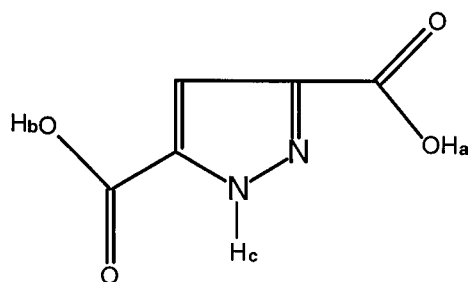
INTRODUCTION

Recent discoveries of new families of porous compounds by the building block approach have sparked considerable interest in designing new functional materials with specified structures and properties (1, 2). Ligands of various binding sites and shapes (including rodlike 4,4'-bipyridine, pyrazine, 1,2-bis(4-pyridyl)ethyne, 1,4-bis(4-pyridyl)butadiyne; triangular 1,3,5-tris(4-ethylbenzotrile)benzene; tetrahedral 1,4,5,8,9,12-hexaazatriphenylene and other multidentate groups such as 5,10,15,20-tetra(pyridyl)porphyrin, adamantane-1,3,5,7-tetracarboxylic acid) have generated numerous extended coordination structures of ladder (3), square net (4), honeycomb (5), brick wall (6), parquet (7), helix (8), and diamondoid (9) networks. Hydrothermal synthesis has been

demonstrated to be an effective and powerful technique for crystal growth of many coordination polymers (10, 11). Unlike several other common routes such as diffusion and silicate gel growth, many inorganic species of low solubility may be used in hydrothermal reactions. While systematic, accurate prediction and total design of a crystal structure are not yet possible, efforts have been made to understand and control certain reaction parameters that play crucial roles in the structure formation processes (12). Our investigation on systems involving carboxylic acid ligands has illustrated that the acidity level of a solution directly affects the reaction products (11f, g). By rational control of pH in a hydrothermal environment, tailored coordination structures may be isolated in high yields. Along this line of research, we have recently succeeded in the selective synthesis of two cadmium-containing three-dimensional coordination frameworks by controlling reaction acidity level. The details of the synthesis and characterization of these compounds are described in this paper.

3,5-Pyrazoledicarboxylic acid (H_3pdc , Scheme 1) as a multidentate ligand has been employed in this study. This ligand possesses three different protonated hydrogens (H_a , H_b , and H_c in Scheme 1). Although both H_a and H_b are attached to carboxylic oxygen atoms, the two experience quite different coordination environments. The H_c in this ligand is linked to a nitrogen atom, and is more difficult to deprotonate than the other two hydrogen atoms. The difference in the binding power of these protons allows us to deprotonate them at different pH levels. The flexible, multifunctional coordination sites of this ligand also give a high likelihood for generation of coordination polymers with high dimensions. Its functional groups (carboxylate and pyrazole ring) bind to metals selectively. For instance, the “harder” lanthanide metals coordinate more preferably to oxygen atoms than to the “softer” nitrogen atoms (13), while the latter show a strong tendency to bind to transition metals. Cadmium is selected as a metal center in this study because of its ambi-ability to form bonds with both nitrogen and oxygen atoms with a d^{10} configuration.

¹ To whom correspondence should be addressed.



SCHEME 1.

EXPERIMENTAL

Materials and instruments. Cadmium(II) nitrate tetrahydrate (99%, Acros), 3,5-pyrazoledicarboxylic acid monohydrate (97%, Acros), and triethylamine (99%+, Alfa Aesar) were used as received without further purification. Thermogravimetric analyses (TGA) were performed under N_2 at a scan rate of $1^\circ\text{C}/\text{min}$ using a computer-controlled TA Instrument TGA 2050 system. Fourier transform infrared (FT-IR) spectra were measured on a photoacoustics Model 300 using a Bio-Rad FTS-6000 IR system.

TABLE 1
Crystallographic Data and Details of Structure Refinement for 1 and 2

		Crystal Data	
Empirical formula	$\text{C}_5\text{H}_4\text{CdN}_2\text{O}_5$ (1)	$\text{C}_{10}\text{H}_6\text{Cd}_3\text{N}_4\text{O}_{10}$ (2)	
Formula weight	284.50	679.39	
Crystal color, habit	Yellowish, blocklike	Yellowish, platelike	
Crystal size	$0.40 \times 0.35 \times 0.25 \text{ mm}^3$	$0.06 \times 0.06 \times 0.01 \text{ mm}^3$	
Crystal system	Monoclinic	Monoclinic	
Space group	$P2_1/c$ (No.14)	$P2_1/c$ (No.14)	
Unit cell parameters	$a = 6.436(1) \text{ \AA}$ $b = 12.283(2) \text{ \AA}$ $c = 8.934(2) \text{ \AA}$ $\beta = 104.23(3)^\circ$	$a = 9.744(2) \text{ \AA}$ $b = 9.821(2) \text{ \AA}$ $c = 7.496(1) \text{ \AA}$ $\beta = 105.23(3)^\circ$	
Volume	$684.6(2) \text{ \AA}^3$	$692.1(2) \text{ \AA}^3$	
Z	4	2	
Density (calculated)	2.760 g/cm^3	3.260 g/cm^3	
Absorption coefficient	3.180 mm^{-1}	4.641 mm^{-1}	
$F(000)$	544	636	
		Data Collection	
Diffractometer	Enraf-Nonius CAD4	Enraf-Nonius CAD4	
Radiation	Graphite-monochromatized $\text{MoK}\alpha$, $\lambda = 0.71073 \text{ \AA}$	Graphite-monochromatized $\text{MoK}\alpha$, $\lambda = 0.71073 \text{ \AA}$	
Temperature	293(2) K	293(2) K	
Data collection range	$2.88^\circ \leq \theta \leq 25.99^\circ$ $0 \leq h \leq 7, 0 \leq k \leq 15, -11 \leq l \leq 10$	$2.17^\circ \leq \theta \leq 25.99^\circ$ $-11 \leq h \leq 11, -12 \leq k \leq 0, 0 \leq l \leq 9$	
Reflections collected	1453	1449	
Independent reflections	1337 ($R_{\text{int}} = 0.0599$)	1351 ($R_{\text{int}} = 0.0759$)	
Scan mode	ω scan	$\omega-2\theta$ scan	
		Solution and Refinement	
Software used	Shelxs97	Shelxs97	
Solution	Direct methods	Direct methods	
Refinement method	Full-matrix least-squares on F^2	Full-matrix least-squares on F^2	
Absorption correction	Empirical Ψ scans	Empirical Ψ scans	
Max and min transmission	0.9997 and 0.6809	0.9951 and 0.8936	
Data/restraints/parameters	1284/0/119	695/0/125	
Final R indices ($I > 2\sigma(I)$)	$R^a = 0.0322, wR^b = 0.0831$	$R^a = 0.0562, wR^b = 0.0846$	
R indices (all data)	$R^a = 0.0339, wR^b = 0.0845$	$R^a = 0.1461, wR^b = 0.0979$	
Weighting scheme	$w = 1/[\sigma^2(F_o^2) + (0.035P)^2 + 4.5P], P = (F_o^2 + 2F_c^2)/3$	$w = 1/[\sigma^2(F_o^2) + (0.01P)^2], P = (F_o^2 + 2F_c^2)/3$	
Goodness-of fit on F^2 ^c	1.155	1.185	
Extinction coefficient	0.072(3)	0.0003(3)	
Largest peak and hole	+ 0.842 to - 1.471 e \AA^{-3}	+ 1.299 to - 1.200 e \AA^{-3}	

$${}^a R1 = \frac{\sum ||F_o| - |F_c||}{\sum |F_o|}, {}^b wR2 = \sqrt{\frac{\sum [w(F_o^2 - F_c^2)^2]}{\sum w(F_o^2)^2}}, {}^c \text{Goof} = S = \sqrt{\frac{\sum [w(F_o^2 - F_c^2)^2]}{(n - p)}}$$

Adsorption is described as usual: very strong (vs), strong (s), medium (m), shoulder (sh), weak (w), and broad (br). Powder X-ray diffraction (PXRD) of samples was measured on a Rigaku D/M-2200T automated diffraction system (Ultima⁺) at an operating power of 40 kV/40 mA. The data were collected at room temperature with a step size of 0.02 in 2θ and a scan speed of 1.7 deg/min. The refinement was carried out using the JADE (Windows) software package. The SHELXTL-XPOW program was used to generate the calculated PXRD pattern from single-crystal data.

Syntheses of ${}^3[Cd(Hpdc)H_2O]$ (1). Hydrothermal reactions of $Cd(NO_3)_2 \cdot 4H_2O$ (0.062 g, 0.2 mmol), $H_3pdc \cdot H_2O$ (0.068 g, 0.4 mmol), and deionized water (10 mL, 0.5555 mol) in a mole ratio of 1 : 2 : 2222 (pH 2.5 in the final solution) in a Teflon-lined bomb at 150°C for 12 days yielded yellowish block crystals of **1** in high yields (0.058 g, 98.1%). IR (4000–400 cm^{-1}): 3498.1(w), 3432.5(m), 3148.2(m), 3068.3(m), 2956.7(m), 2886.6(m), 2719.1(m), 2659.9(m), 2544.3(m), 2478.1(m), 2385.6(m), 2225.6(m), 1732.7(m), 1637.6(sh), 1558.4(vs), 1520.6(m), 1451.4(s), 1373.1(s), 1272.2(w), 1209.7(s), 1114.1(m), 1029.3(s), 869.5(sh), 846.5(sh), 800.3(s), 678.2(m), 646.6(m), 531.4(s). The purity of the bulk sample was confirmed by PXRD analysis.

Synthesis of ${}^3[Cd_3(pdc)_2(H_2O)_2]$ (2). Reactions of $Cd(NO_3)_2 \cdot 4H_2O$ (0.155 g, 0.5 mmol), $H_3pdc \cdot H_2O$ (0.043 g, 0.25 mol), Et_3N (0.07 mL, 0.5 mmol), and deionized water (10 mL, 0.5555 mol) in a mole ratio of 2 : 1 : 2 : 2222 in a Teflon-lined bomb at 150°C for 11 days produced pale yellowish plate crystals of **2** (0.072 g, 63.7%) in solution (pH 4). IR (400–4000 cm^{-1}): 3180–3140(br), 2294.2(m), 2213.4(m), 1709.7(m), 1647.3(m), 1586.8(sh), 1539.7(vs), 1489.5(vs), 1388.2(sh), 1304.3(vs), 1156.8(s), 1062.9(m), 1015.8(m), 887.7(w), 829.7(sh), 795.2(s), 731.5(w), 655.8(s), 556.8(m). The sample was isolated as a single-phase material.

Crystallographic studies. The room temperature (293 ± 1 K) single-crystal X-ray diffraction experiments were performed on an Enraf-Nonius CAD4 diffractometer equipped with graphite-monochromatized $MoK\alpha$ radiation. A yellowish blocklike crystal of **1** and a platelike crystal of **2** with approximate dimensions 0.40 × 0.35 × 0.25 and 0.06 × 0.06 × 0.01 mm³, respectively, were mounted on the tips of glass fibers and placed onto the goniometer head. Unit cells were obtained and refined by 20 well-centered reflections with $13.63^\circ \leq \theta \leq 18.28^\circ$ for **1** and 25 well-centered reflections with $6.11^\circ \leq \theta \leq 11.64^\circ$ for **2**. Data collection was monitored by three standards every 2 hours. No decay was observed except the statistic fluctuation in the range of ±1.2% (**1**) and ±2.3% (**2**), respectively. Raw intensities were corrected for Lorentz and polarization effects, and for absorption by empirical method based on ψ -scan data (14). Direct phase determination yielded the positions of Cd atoms. The remaining nonhydrogen atoms

were located from the subsequent difference Fourier synthesis. Hydrogen atoms were located from difference Fourier map and their thermal parameters were set equal to $1.2U_{eq}$ of the parent nonhydrogen atoms. All nonhydrogen atoms were subjected to anisotropic refinement. An extinction correction was applied and refined to 0.072(3) for **1** and 0.0003(3) for **2**, respectively (15). The final full-matrix least-squares refinement on F^2 converged with $R1 = 0.0322$ and $wR2 = 0.0831$ for 1284 observed reflections ($I > 2\sigma(I)$) for **1** and $R1 = 0.0562$ and $wR2 = 0.0846$ for 695 observed reflections ($I > 2\sigma(I)$) for **2**. The largest shift/esd values in the final cycle of refinement were 0.000 (**1**) and 0.001 (**2**). The largest peak in the final difference Fourier map was 1.299 $e/\text{\AA}^3$ and 0.842 $e/\text{\AA}^3$ for **1** and **2**, respectively. Details of data collection and structure refinement, along with crystal parameters, are given in Table 1. Data collection was controlled by the CAD4/PC program package. Computations were performed using the SHELX97 program package (16) on a PC586 system. Analytic expressions of atomic scattering factors were employed, and anomalous dispersion corrections were incorporated (17). Crystal drawings were produced with SCHAKAL 92 (18). Final atomic coordinates and average temperature factors are listed in Tables 2 and 3, and selected bond lengths and angles are reported in Tables 4 and 5.

RESULTS AND DISCUSSION

The hydrothermal reactions of $Cd(NO_3)_2$ and 3,5-pyrazoledicarboxylic acid (H_3pdc) at different pH levels have

TABLE 2
Atomic Coordinates and Equivalent Isotropic Temperature Factors^a (\AA^2) for **1**

Atoms	x	y	z	U (eq)
Cd	0.7539(1)	0.6678(1)	0.1208(1)	0.016(1)
O(1)	0.7427(6)	0.7119(3)	0.3817(4)	0.025(1)
O(2)	0.7587(5)	0.6469(3)	0.6133(4)	0.020(1)
O(3)	0.8724(6)	0.1761(3)	0.3153(5)	0.025(1)
O(4)	0.6231(6)	0.1795(3)	0.4472(5)	0.022(1)
O(5)	0.7655(7)	0.5574(3)	−0.0855(5)	0.034(1)
N(1)	0.7491(6)	0.5093(3)	0.2621(5)	0.017(1)
N(2)	0.7504(7)	0.4023(3)	0.2395(5)	0.017(1)
C(1)	0.7481(7)	0.6334(4)	0.4722(6)	0.016(1)
C(2)	0.7424(7)	0.5222(4)	0.4101(5)	0.015(1)
C(3)	0.7327(8)	0.4219(4)	0.4801(5)	0.016(1)
C(4)	0.7388(7)	0.3462(4)	0.3678(5)	0.015(1)
C(5)	0.7446(7)	0.2253(4)	0.3759(5)	0.015(1)
H(1)	0.7436	0.5713	−0.1899	0.041
H(2)	0.7573	0.4821	−0.1018	0.041
H(3)	0.7405	0.3688	0.1528	0.020
H(4)	0.7335	0.4064	0.5800	0.019

^a U_{eq} defined as one-third of the trace of the orthogonalized U tensor.

TABLE 3
Atomic Coordinates and Equivalent Isotropic Temperature Factors^a (Å²) for **2**

Atoms	x	y	z	U (eq)
Cd(1)	0	0	0	0.016(1)
Cd(2)	0.2764(1)	0.0081(2)	0.4439(1)	0.015(1)
O(1)	0.1651(10)	0.2114(10)	0.4891(14)	0.020(3)
O(2)	0.2112(11)	0.4121(11)	0.6280(15)	0.019(3)
O(3)	0.8618(10)	0.3307(11)	0.5927(14)	0.019(3)
O(4)	0.8016(11)	0.4629(10)	0.7913(14)	0.022(3)
O(5)	0.0450(10)	-0.0783(10)	0.3066(12)	0.016(2)
N(1)	0.4550(13)	0.1582(12)	0.5649(17)	0.013(3)
N(2)	0.5979(14)	0.1772(12)	0.5909(17)	0.015(3)
C(1)	0.2479(16)	0.3013(14)	0.5690(2)	0.016(3)
C(2)	0.4011(14)	0.2811(15)	0.5961(19)	0.011(3)
C(3)	0.5122(15)	0.3728(14)	0.6590(2)	0.014(3)
C(4)	0.6308(15)	0.3048(15)	0.6425(19)	0.014(3)
C(5)	0.7764(15)	0.3645(14)	0.6776(18)	0.013(3)
H(1)	-0.0357	-0.0571	0.3322	0.019
H(2)	0.0622	-0.1736	0.2944	0.019
H(3)	0.4947	0.4915	0.6441	0.017

^a U_{eq} defined as one-third of the trace of the orthogonalized **U** tensor.

TABLE 4
Selected Bond Lengths (Å) and Bond Angles (°) for **1**

Cd–O(2) ⁱ	2.278(4)	Cd–O(1) ⁱ	2.584(4)
Cd–O(5)	2.304(4)	O(1)–Cd ^{iv}	2.584(4)
Cd–N(1)	2.324(4)	O(2)–Cd ^{iv}	2.278(4)
Cd–O(3) ⁱⁱ	2.334(4)	O(3)–Cd ^v	2.334(4)
Cd–O(4) ⁱⁱⁱ	2.357(4)	O(4)–Cd ^{vi}	2.357(4)
Cd–O(1)	2.411(3)		
O(2) ^j –Cd–O(5)	124.12(14)	O(5)–Cd–O(1)	156.95(15)
O(2) ^j –Cd–N(1)	148.76(13)	N(1)–Cd–O(1)	69.85(14)
O(5)–Cd–N(1)	87.10(14)	O(3) ⁱⁱ –Cd–O(1)	91.59(15)
O(2) ^j –Cd–O(3) ⁱⁱ	86.73(12)	O(4) ⁱⁱⁱ –Cd–O(1)	87.80(13)
O(5)–Cd–O(3) ⁱⁱ	89.28(16)	O(2) ^j –Cd–O(1) ⁱ	53.26(12)
N(1)–Cd–O(3) ⁱⁱ	93.11(14)	O(5)–Cd–O(1) ⁱ	71.03(14)
O(2) ^j –Cd–O(4) ⁱⁱⁱ	87.24(12)	N(1)–Cd–O(1) ⁱ	157.91(13)
O(5)–Cd–O(4) ⁱⁱⁱ	93.65(15)	O(3) ⁱⁱ –Cd–O(1) ⁱ	89.72(13)
N(1)–Cd–O(4) ⁱⁱⁱ	92.34(14)	O(4) ⁱⁱⁱ –Cd–O(1) ⁱ	86.22(13)
O(3) ⁱⁱ –Cd–O(4) ⁱⁱⁱ	173.94(13)	O(1)–Cd–O(1) ⁱ	132.00(4)
O(2) ^j –Cd–O(1)	78.92(13)	Cd–O(1)–Cd ^{iv}	157.86(17)

Note. Symmetry transformations used to generate equivalent atoms: i, x, -y + 3/2, z - 1/2; ii, -x + 2, y + 1/2, -z + 1/2; iii, -x + 1, y + 1/2, -z + 1/2; iv, x, -y + 3/2, z + 1/2; v, -x + 2, y - 1/2, -z + 1/2; vi, -x + 1, y - 1/2, -z + 1/2.

afforded two three-dimensional cadmium coordination polymers with empirical formulas of ${}^3_{\infty}[\text{Cd}(\text{Hpdc})(\text{H}_2\text{O})]$ (**1**) and ${}^3_{\infty}[\text{Cd}_3(\text{pdc})_2(\text{H}_2\text{O})_2]$ (**2**). The ORTEP drawing of **1** is illustrated in Fig. 1a. The local coordination environment around a cadmium metal center can be best described as pentagonal bipyramid (Fig. 1b). The pentagonal plane is composed of two chelating Hpdc^{2-} , one via two oxygen atoms of a carboxylate (O1ⁱ and O2ⁱ) and the other via an oxygen of a carboxylate (O1) and its adjacent nitrogen atom (N1), and a fifth site, by a water molecule (H₂O). The apical sites are taken by two monodentate carboxylate ions. Each cadmium atom is bridged through O1, O2, and N1 of an

Hpdc^{2-} and O1ⁱ, O2ⁱ, and N1ⁱ of the other to form a zigzag chain (or more precisely, ribbon) running parallel to the *c*-axis, as shown in Fig. 2. The inter-ribbon connections are made through O3 and O4 atoms (and O3ⁱ and O4ⁱ) which coordinate to one Cd above and another Cd below the plane of the chain in an *anti-anti* mode (19). This results in the three-dimensional structure plotted in Fig. 3. The simplified top view emphasizes the connectivity among the zigzag ribbons by showing only the metal atoms and the carboxylate ions containing O3/O4 (and O3ⁱ/O4ⁱ). The bottom view is the actual 3D network along the *c*-axis. The

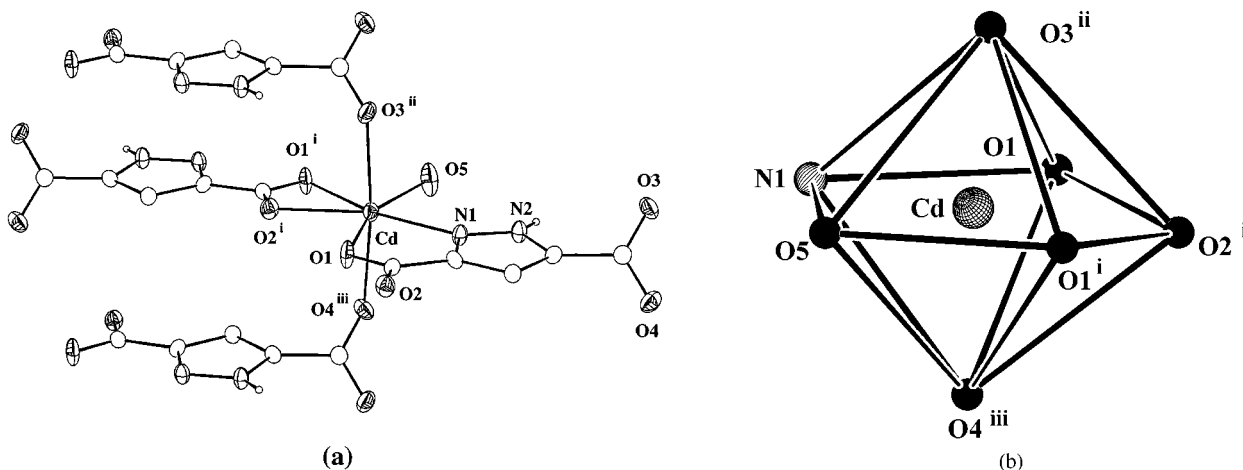


FIG. 1. (a) ORTEP drawing of **1** with thermal vibrational ellipsoids (50%). (b) Pentagonal bipyramidal polyhedron showing the seven-fold coordination of a cadmium metal center in **1**. Cross-shaded circles are metal atoms; solid and shaded circles are O and N atoms, respectively.

TABLE 5
Selected Bond Lengths (Å) and Bond Angles (°) for **2**

Cd(1)–O(2) ⁱ	2.205(10)	Cd(2)–O(4) ^{vii}	2.347(10)
Cd(1)–O(2) ⁱⁱ	2.205(10)	Cd(2)–O(5)	2.376(9)
Cd(1)–O(5) ⁱⁱⁱ	2.353(9)	Cd(2)–O(2) ⁱ	2.415(11)
Cd(1)–O(5)	2.353(9)	O(2)–Cd(1) ^{viii}	2.205(10)
Cd(1)–O(3) ^{iv}	2.356(10)	O(2)–Cd(2) ^{ix}	2.415(11)
Cd(1)–O(3) ^v	2.356(10)	O(3)–Cd(1) ^x	2.356(10)
Cd(2)–N(2) ^{vi}	2.246(13)	O(4)–Cd(2) ^{xi}	2.347(10)
Cd(2)–N(1)	2.280(12)	N(2)–Cd(2) ^{vi}	2.246(13)
Cd(2)–O(1)	2.339(10)		
O(2) ⁱ –Cd(1)–O(2) ⁱⁱ	180.0	N(2) ^{vi} –Cd(2)–O(1)	174.8(4)
O(2) ⁱ –Cd(1)–O(5) ⁱⁱⁱ	102.1(3)	N(1)–Cd(2)–O(1)	74.0(4)
O(2) ⁱⁱ –Cd(1)–O(5) ⁱⁱⁱ	77.9(3)	N(2) ^{vi} –Cd(2)–O(4) ^{vii}	104.6(4)
O(2) ⁱ –Cd(1)–O(5)	77.9(3)	N(1)–Cd(2)–O(4) ^{vii}	99.7(4)
O(2) ⁱⁱ –Cd(1)–O(5)	102.1(3)	O(1)–Cd(2)–O(4) ^{vii}	76.9(4)
O(5) ⁱⁱⁱ –Cd(1)–O(5)	180.0	N(2) ^{vi} –Cd(2)–O(5)	98.3(4)
O(2) ⁱ –Cd(1)–O(3) ^{iv}	97.8(4)	N(1)–Cd(2)–O(5)	160.4(4)
O(2) ⁱⁱ –Cd(1)–O(3) ^{iv}	82.2(4)	O(1)–Cd(2)–O(5)	86.8(3)
O(5) ⁱⁱⁱ –Cd(1)–O(3) ^{iv}	94.8(4)	O(4) ^{vii} –Cd(2)–O(5)	79.5(3)
O(5)–Cd(1)–O(3) ^{iv}	85.2(4)	N(2) ^{vi} –Cd(2)–O(2) ⁱ	99.2(4)
O(2) ⁱ –Cd(1)–O(3) ^v	82.2(4)	N(1)–Cd(2)–O(2) ⁱ	99.0(4)
O(2) ⁱⁱ –Cd(1)–O(3) ^v	97.8(4)	O(1)–Cd(2)–O(2) ⁱ	81.5(4)
O(5) ⁱⁱⁱ –Cd(1)–O(3) ^v	85.2(4)	O(4) ^{vii} –Cd(2)–O(2) ⁱ	146.2(3)
O(5)–Cd(1)–O(3) ^v	94.8(4)	O(5)–Cd(2)–O(2) ⁱ	73.5(3)
O(3) ^{iv} –Cd(1)–O(3) ^v	180.0	Cd(1) ^{viii} –O(2)–Cd(2) ^{ix}	105.9(4)
N(2) ^{vi} –Cd(2)–N(1)	100.8(4)	Cd(1)–O(5)–Cd(2)	102.6(4)

Note. Symmetry transformations used to generate equivalent atoms: i, $x, -y + 1/2, z - 1/2$; ii, $-x, y - 1/2, -z + 1/2$; iii, $-x, -y, -z$; iv, $x - 1, -y + 1/2, z - 1/2$; v, $-x + 1, y - 1/2, -z + 1/2$; vi, $-x + 1, -y, -z + 1$; vii, $-x + 1, y - 1/2, -z + 3/2$; viii, $-x, y + 1/2, -z + 1/2$; ix, $x, -y + 1/2, z + 1/2x - x + 1, y + 1/2, -z + 1/2$; xi, $-x + 1, y + 1/2, -z + 3/2$.

nearest Cd–Cd distance in the zigzag chain is 4.90 Å, whereas the two Cd atoms bridged by O3 and O4 of the same carboxylate (*anti-anti* mode) are 6.44 Å apart (the length of *a*-axis). The connectivity among the metal centers is depicted in Fig. 4, which clearly shows that all metals are six-connected. The topological relation to that of α -Po is clearly seen (20). All Cd–O interatomic distances (2.278(4)–2.411(3) Å) in **1** fall in the normal range of cadmium–oxygen bond lengths (2.227–2.525 Å) (21). Note that Cd–O1ⁱ (2.584(4) Å) and Cd–O1 (2.411(3) Å) are somewhat longer than other Cd–O bonds, due to its μ_2 -coordination mode (Fig. 2). The O3ⁱⁱ–Cd–O4ⁱⁱⁱ angle is 173.94(13)°, and O1ⁱ–Cd–O2ⁱ and O1–Cd–N1 angles are 53.26(12) and 69.85(14)°, respectively.

Structure **2** differs significantly from **1**. Deprotonation of the hydrogen bonded to the pyrazole nitrogen was made possible by adjusting the pH level of the solution through addition of triethylamine to the reaction. The resultant structure contains solely pdc^{3-} rather than Hpdc^{2-} in **1**. There are two crystallographic independent cadmium atoms; both are six-coordinated and their local coordina-

tion geometries can be approximately described as distorted octahedra. As shown in Fig. 5, Cd1 is located at an inversion center while Cd2 resides at a general position. Cd1 coordinates to four pdc^{3-} , each through a single carboxylate oxygen. The remaining two sites are occupied by two water molecules. Cd2 bonds to two monodentate pdc^{3-} , each also via a single carboxylate oxygen; a chelating pdc^{3-} via a carboxylate oxygen and its adjacent nitrogen; a fourth pdc^{3-} via one of its pyrazole nitrogen; and a water molecule. The

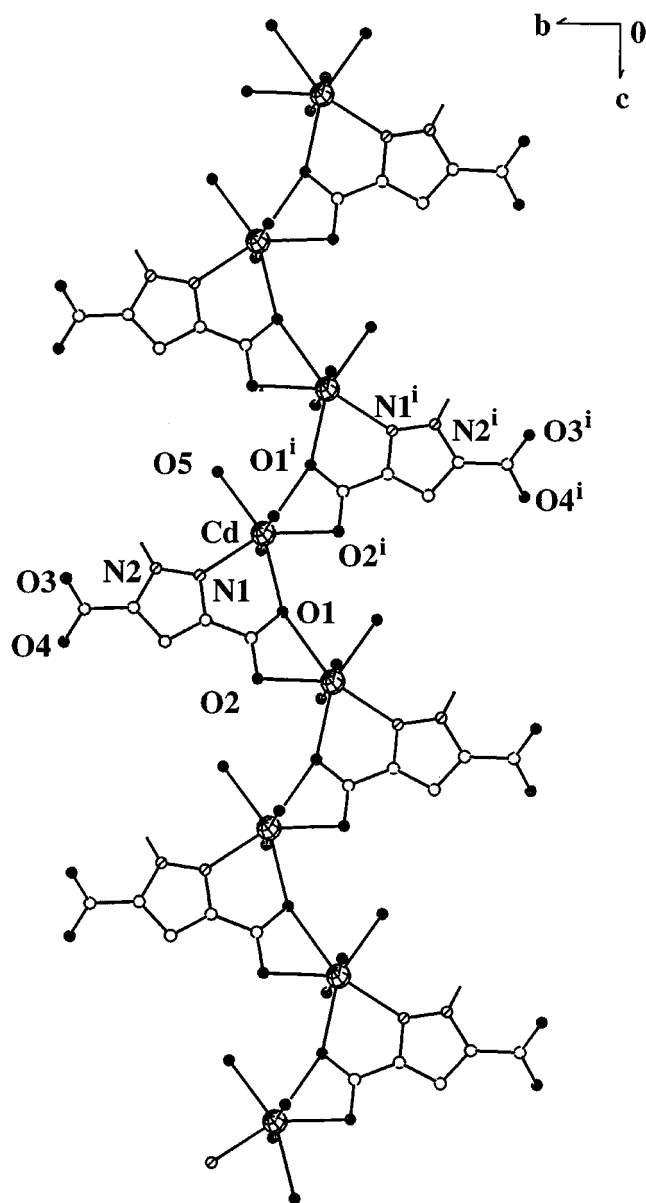


FIG. 2. One-dimensional zigzag chain of $[\text{Cd}(\text{Hpdc})(\text{H}_2\text{O})]$ in **1** running along the *c*-axis. Note that the uncoordinated carboxylate oxygen atoms (e.g., O3, O4, O3ⁱ, and O4ⁱ) are out of the plane of the chain (or ribbon). The same labeling scheme as in Fig. 1 is used. The open circles represent C atoms.

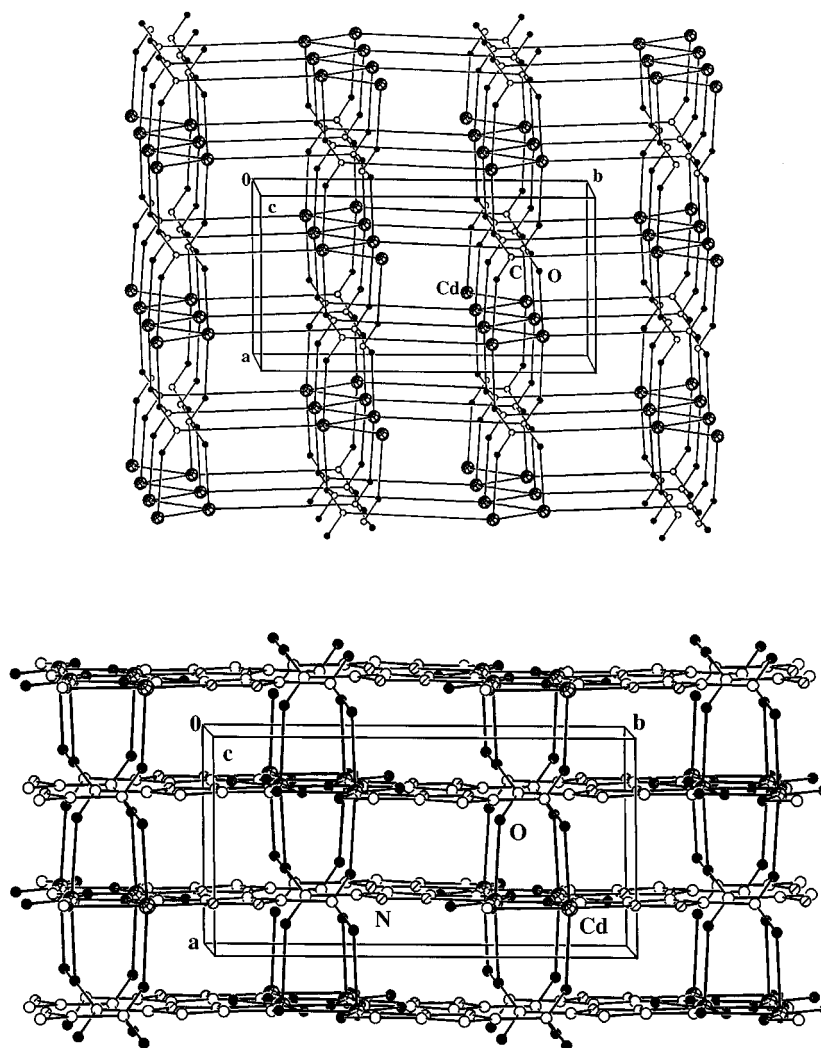


FIG. 3. Views of the three-dimensional network of **1**. The top view is a simplified version of the actual structure emphasizing the connectivity between the one-dimensional chains. Only the metal centers and the carboxylate ions that bridge the chains are shown. The bottom view is the actual 3D crystal structure. Both views are shown along the same direction (*c*-axis). The same labeling scheme as in Fig. 2 is used.

Cd1–O (2.205(10)–2.356(10) Å) and Cd2–O bonds (2.239(10)–2.415(11) Å) and the corresponding bond angles compare well with those reported (22). The overall crystal structure of **2** viewing along the *b*-axis is presented in Fig. 6. The metals form a three-layer slab (Cd2–Cd1–Cd2) in which Cd1 resides in the central layer and are connected to Cd2 in the layers above and below by a μ_2 -oxygen of a coordinated water molecule and a μ_2 -oxygen of carboxylate ion. These slabs are bridged through the pdc^{3-} which connects the Cd atoms in the neighboring slabs via its two pyrazole nitrogen atoms and all four carboxylate oxygens to result in a three-dimensional network (Figs. 6 and 7). The shortest separation between the two Cd2 atoms in the neighboring slabs is 4.22 Å. To help understand the structure, Fig. 8 shows the two structure motifs with (a) removal of all Cd2 atoms and

a one-dimensional $\frac{1}{\infty}[\text{Cd1}(\text{pdc})_2(\text{H}_2\text{O})_2]$ chain in (a) and a two-dimensional $\frac{2}{\infty}[(\text{Cd2})_2(\text{pdc})_2(\text{H}_2\text{O})_2]$ layer in (b). The metal connectivity is depicted in Fig. 9, giving a topology similar to that shown in Fig. 4. All Cd1 atoms are two-connected to Cd2 (one above and one below the Cd1 plane) with a distance of 3.69 Å and four-connected to Cd1 in the same metal plane (6.18 Å). All Cd2 atoms are six-connected, four to Cd2 in the same plane (6.05, 6.30 Å), one to Cd2 in the neighboring plane (4.22 Å), and one to Cd1 from the neighboring plane of the opposite side (3.69 Å).

The role of the multidentate 3,5-pyrazoledicarboxylate ligand in the final choice of a crystal structure is apparent. This ligand has demonstrated versatile coordination modes during the formation of numerous coordination frameworks. Seven different coordination modes of H_3pdc have been observed in a series of lanthanide coordination

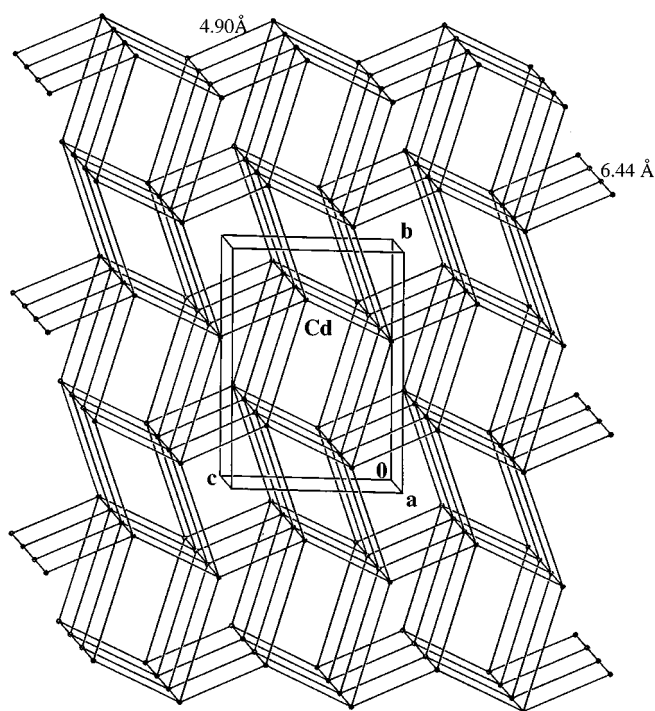


FIG. 4. View along the *a*-axis showing the connectivity among the metal atoms in **1**. Each Cd is six-fold connected to other metals. The shortest Cd–Cd distances are 4.90 Å (two nearest neighboring Cd atoms in the zigzag chain) and 6.44 Å (two Cd atoms bridged by O3 and O4 of the same carboxylate).

frameworks that we reported earlier (11f), including three (one μ_4 and two different μ_5) in the three-dimensional structure ${}^3_{\infty}[\text{Ln}_2(\text{Hpdc})_3(\text{H}_2\text{O})_4] \cdot 2\text{H}_2\text{O}$ ($\text{Ln} = \text{La}, \text{Ce}$), two (μ_2 and μ_4) in the double-layer structure ${}^2_{\infty}[\text{Ln}_2(\text{Hpdc})_3(\text{H}_2\text{O})_6]$ ($\text{Ln} = \text{Eu}, \text{Er}$), and two (different μ_3) in the single-layer structure ${}^2_{\infty}[\text{Ln}(\text{Hpdc})(\text{H}_2\text{pdc})(\text{H}_2\text{O})_2]$ ($\text{Ln} = \text{Er}, \text{Lu}$) as shown in Scheme 2. As a comparison, the coordination modes of this ligand in the title compounds are also shown in Scheme 2. In structure **1**, four metal centers are linked to it through μ_6 -bridging, whereas it utilizes a μ_7 -bridging mode in structure **2** to bind six metal centers. Both are different from what have been observed in the lanthanide compounds. Compared to the rare-earth series, the title compounds possess a higher connectivity (μ_6 and μ_7) due to the dual coordination ability of the Cd atoms toward both O and N in the carboxylate and pyrazole functional groups of the ligand. An even higher coordination mode of H_3pdc to Cd has been found in other cadmium framework structures where a μ_8 -bridging ligand is identified (23).

Our previous studies on rare-earth metal coordination compounds involving 3,5-pyrazoledicarboxylic acid as ligand (11f) showed that H_3pdc is very sensitive to the pH level as well as to the metals with different coordination

habit. By adjusting the amount of H_2pdc^- and Hpdc^{2-} via concentration change of Et_3N and HNO_3 in the solution, we succeeded in phase separation of the single- and double-layer structures. However, an attempt to deprotonate the H atom bonded to pyrazole nitrogen was not successful. In the cadmium system, this has been achieved for **2**. In order to understand the influence of the reaction pH, we have conducted a series of reactions with various experimental conditions that are summarized in Table 6.

It is clear from Table 6 that the formation of **1** and **2** was largely dependent on the acidity level of the reactions.

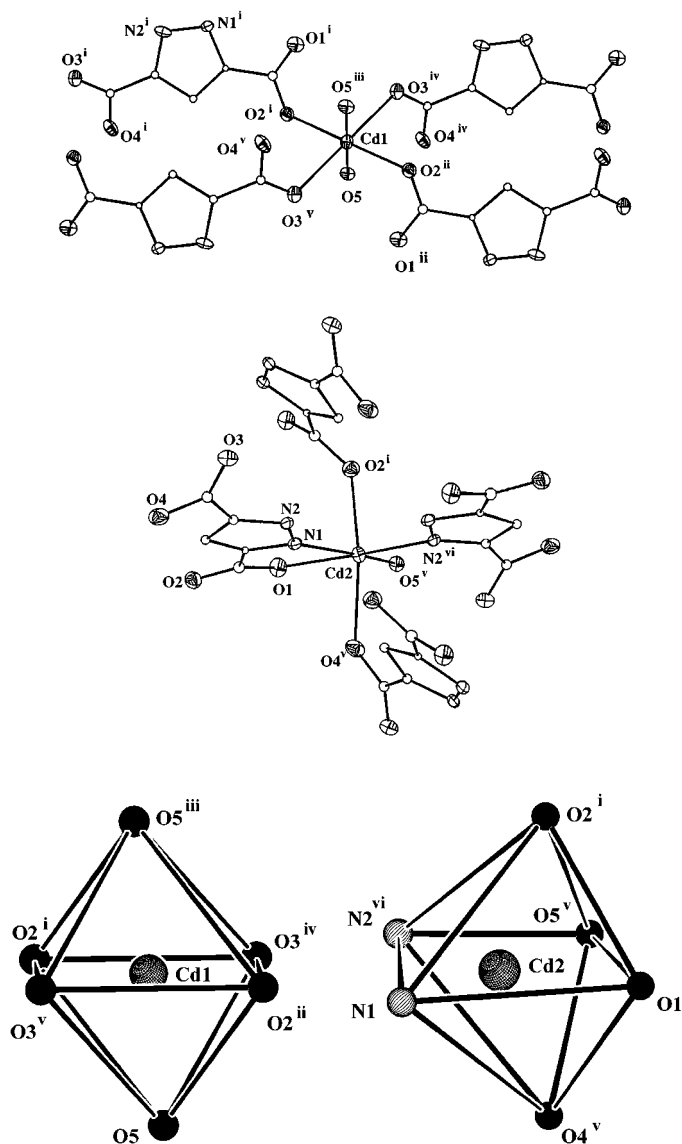


FIG. 5. (Top) Two ORTEP drawings of **2** with thermal vibrational ellipsoids (50%) showing the coordination geometry of Cd1 and Cd2. (Bottom) Polyhedra around the metal atoms. Both Cd1 and Cd2 have distorted octahedral coordination. Cross-shaded circles are metal atoms, Solid and shaded circles are O and N atoms, respectively.

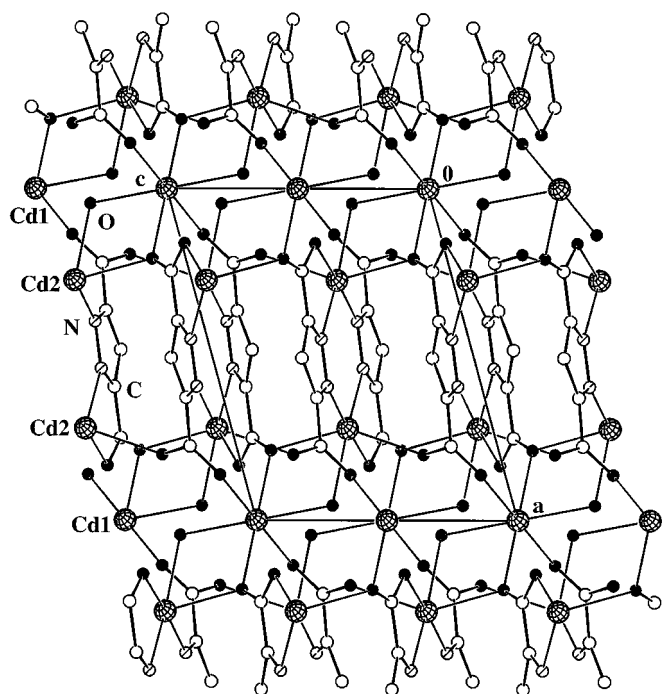


FIG. 6. View of **2** along the *b*-axis. Two three-layer metal slabs (Cd2–Cd1–Cd2) are shown in the figure. The same labeling scheme as in Fig. 5 is used. Open circles represent C atoms.

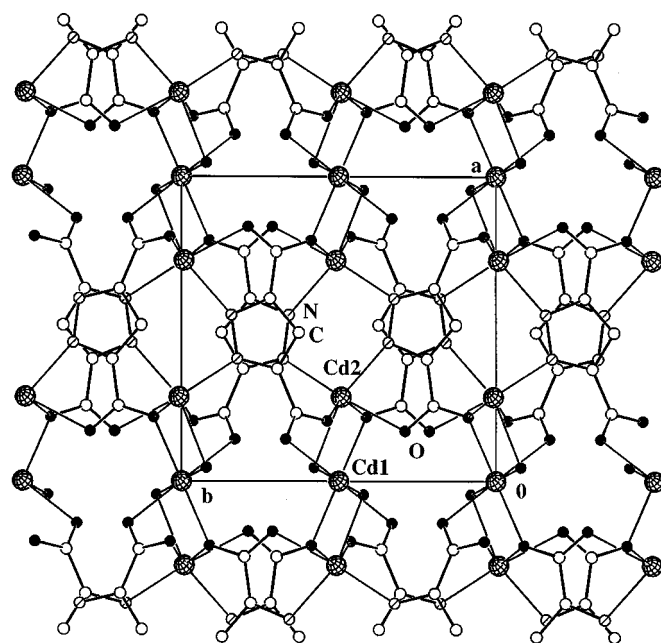
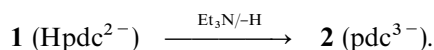


FIG. 7. View of **2** along the *c*-axis. The three-layer metal slabs are bridged through pdc^{3-} via its carboxylate and pyrazole functional groups. The same labeling scheme as in Fig. 6 is used.

Addition of Et_3N (a base) to increase the pH value led to conversion of **1** to **2**:



Based on the soft and hard acid and base theory, cadmium metal is a softer acid than rare-earth metals. Its preference and high ability to coordinate to both pyrazole nitrogen atoms drives the above equation to the right side and makes it possible to isolate single-phase compound **2**.

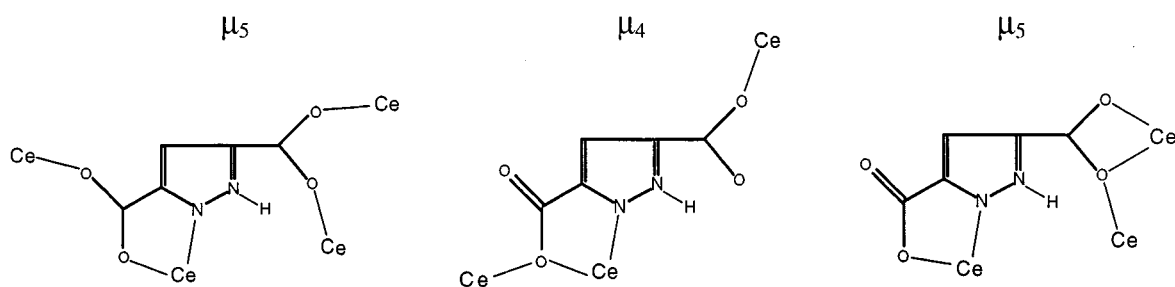
The IR spectra indicated the asymmetric vibration $\nu_{\text{as}}\text{C}(\text{COO}^-)$ around 1558 cm^{-1} for **1** and 1540 cm^{-1} for **2**,

respectively (**24**). It is worth noting that the stretching vibrations at $3498\text{--}3432\text{ cm}^{-1}$ assigned to secondary aromatic amine ($\nu = \text{N-H}$) are clearly observed in structure **1**; however, they are absent in structure **2**. This observation confirms that the hydrogen attached to the pyrazole nitrogen is deprotonated (**25**) and is consistent with the result from single-crystal X-ray analysis. Both **1** and **2** do not dissolve in common solvents such as benzene, diethyl ether, acetonitrile, *N,N'*-dimethylformamide (DMF), and dimethyl sulfoxide (DMSO). The thermal behaviors of both compounds were examined by thermogravimetric analysis (TGA). Losses of coordinated water molecules were observed

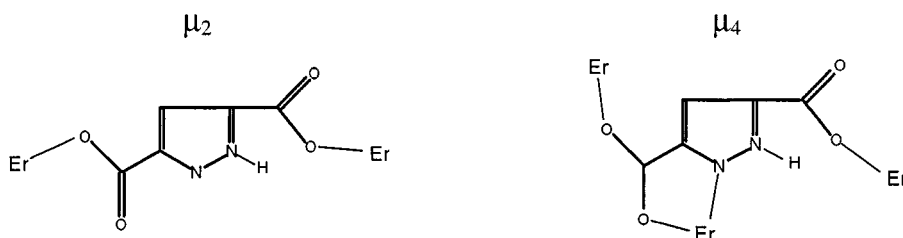
TABLE 6
Experimental Variables and Products for a Set of Planned Reactions (Temp 150°C)

Expt. parameter	Reaction no.									
	1	2	3	4	5	6	7	8	9	10
$\text{Cd}(\text{NO}_3)_2 \cdot \text{H}_2\text{O}$ (mmol)	0.25	0.25	0.25	0.25	0.25	0.2	0.4	0.8	0.1	0.1
H_3pdc (mmol)	0.25	0.25	0.25	0.25	0.25	0.1	0.1	0.1	0.2	0.4
Et_3N (mmol)	0.2	0.3	0.4	0.5	0.8	—	—	—	—	—
H_2O (mL)	10	10	10	10	10	12	12	12	10	10
pH (initial solution)			6.2–6.6				4.2–4.5			
pH (final solution)	3.5	4.0	5.0	5.5	6.0	2.5	2.5	2.5	2.5	2.5
Time (day)	12	12	12	12	12	6	6	6	12	12
Product	2	2	2	2	2	1	1	1	1	1

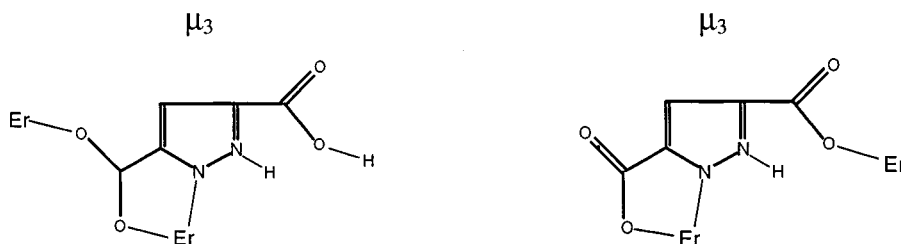
[Ln₂(Hpdc)₃(H₂O)₄]·2H₂O, Ln = La, Ce (three-dimensional network)



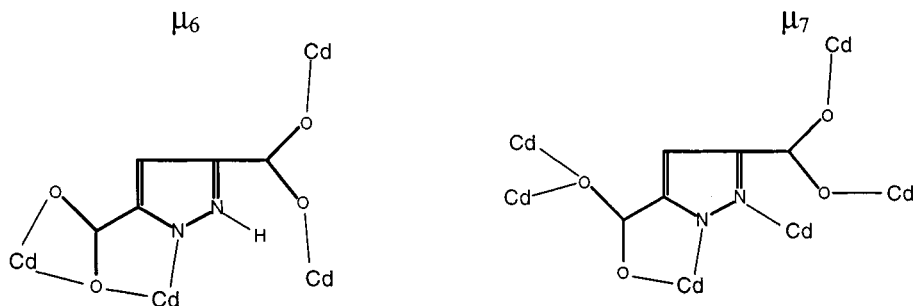
[Ln₂(Hpdc)₃(H₂O)₆], Ln = Eu, Er (double-layer network)



[Ln(Hpdc)(H₂pdc)(H₂O)₂], Ln = Er, Lu (single-layer network)



[Cd(Hpdc)(H₂O)] (1) and [Cd₃(pdc)₂(H₂O)₂] (2)



SCHEME 2.

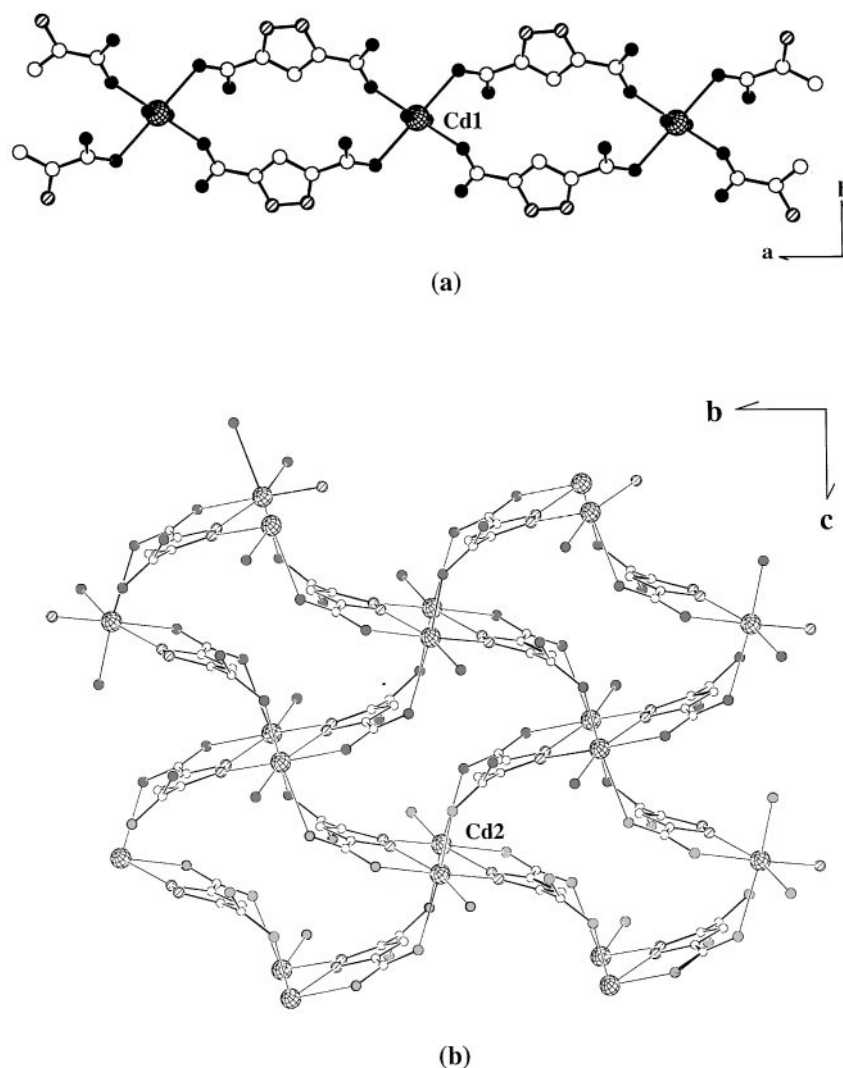


FIG. 8. Views of two structure motifs of **2**. (a) $\frac{1}{2}[\text{Cd1}(\text{pdc})_2(\text{H}_2\text{O})_2]$ one-dimensional chain along the c -axis. (b) $\frac{1}{2}[(\text{Cd2})_2(\text{pdc})_2(\text{H}_2\text{O})_2]$ two-dimensional layer along the a -axis. The same labeling scheme as in Fig. 6 is used.

around 213°C and 179°C, respectively, for **1** and **2**. The 3,5-pyrazoledicarboxylate ligand began to lose at ~271°C and 288°C and the decomposition processes were completed at approximately 620°C for **1** and 480°C for **2**, respectively. The narrow step for the water loss of the two compounds limits the application of the re-adsorption procedure. PXRD analysis revealed that CdO is the final residue of the thermal decomposition for both compounds.

CONCLUSIONS

In this paper, we have described the synthesis and phase separation of two three-dimensional cadmium coordination

compounds in hydrothermal solutions. While use of a complex, multidentate 3,5-pyrazoledicarboxylate ligand may appear to complicate the structure design process, the flexibility of the coordination mode of this ligand provides us with a larger degree of freedom to probe its change with various reaction conditions such as pH value and metal centers. By controlling the acidity level, deprotonation may occur at three levels, $\text{H}_3\text{pdc} \rightarrow \text{H}_2\text{pdc}^- + \text{H}^+ \rightarrow \text{Hpdc}^2 + 2\text{H}^+ \rightarrow \text{pdc}^{3-} + 3\text{H}^+$, and different products result. The successful isolation and phase separation of these compounds have demonstrated that rational control of pH level is an important factor during structure formation which may provide effective means in rational synthesis of new coordination polymers.

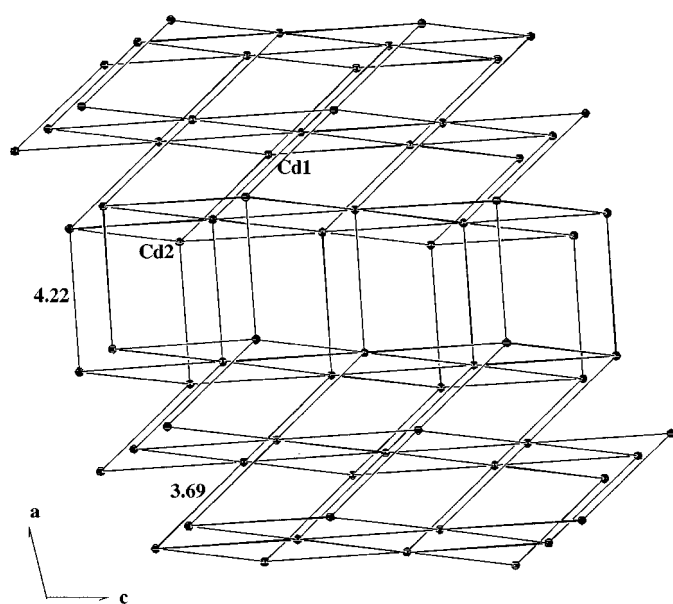


FIG. 9. View along the b -axis showing the connectivity among the metal atoms in **2**. Each Cd is six-fold connected to other metals (Cd1 to two Cd2 and four Cd1, Cd2 to one Cd1 and five Cd2). The shortest Cd1–Cd2 (in the same slab) and Cd2–Cd2 (from the neighboring slabs) distances are 3.69 Å and 4.22 Å, respectively.

ACKNOWLEDGMENTS

Financial support from the National Science Foundation (DMR-9553066) is gratefully acknowledged. The FT-IR/TGA/DSC apparatus was purchased through an NSF ARI grant (CHE 9601710-ARI).

REFERENCES

- H. Gudbjartson, K. Biradha, K. M. Poirier, and M. J. Zaworotko, *J. Am. Chem. Soc.* **121**, 2599 (1999); L. Carlucci, G. Ciani, P. Macchi, and D. M. Proserpio, *J. Chem. Soc., Chem. Commun.* 1837 (1998); A. J. Blake, N. R. Champness, A. Khlobystov, D. A. Lemenovskii, W.-S. Li, and M. Schröder, *J. Chem. Soc., Chem. Commun.* 2027 (1997); B. F. Abrahams, P. A. Jackson, and R. Robson, *Angew. Chem., Int. Ed.* **37**, 2656 (1998); L. Carlucci, G. Ciani, D. M. Proserpio, and A. Sironi, *J. Am. Chem. Soc.* **117**, 12861 (1995).
- I. W. C. E. Arends, R. A. Sheldon, M. Wallau, and U. Schuchardt, *Angew. Chem., Int. Ed. Engl.* **36**, 1144 (1997); J. Y. Ying, C. P. Mehnert, and M. S. Wong, *Angew. Chem., Int. Ed. Engl.* **38**, 56 (1999); H. Zhang, X. Wang, B. K. Teo, *J. Am. Chem. Soc.* **118**, 6307 (1996); T. M. Reineke, M. Eddaoudi, M. Fehr, D. Kelley, and O. M. Yaghi, *J. Am. Chem. Soc.* **121**, 165 (1999).
- T. L. Hennigar, D. C. MacQuarrie, P. Losier, R. D. Rogers, and M. J. Zaworotko, *Angew. Chem., Int. Ed. Engl.* **36**, 972 (1997).
- R. W. Gable, B. F. Hoskins, and R. Robson, *J. Chem. Soc., Chem. Commun.* 1677 (1990).
- G. B. Gardner, D. Venkataraman, J. S. Moore, and S. Lee, *Nature* **374**, 792 (1995); Y.-H. Kiang, G. B. Gardner, S. Lee, Z. Xu, and E. B. Lobkovsky, *J. Am. Chem. Soc.* **121**, 8204 (1999).
- M. Fujita, Y. J. Kwon, O. Sasaki, K. Yamaguchi, and K. Ogura, *J. Am. Chem. Soc.* **117**, 7287 (1995).
- L. Carlucci, G. Ciani, and D. M. Proserpio, *J. Chem. Soc., Dalton Trans.* 1799 (1999); Y. B. Dong, R. C. Layland, N. G. Pschirer, M. D. Smith, U. H. F. Bunz, and H.-C. zur Loye, *Chem. Mater.* **11**, 1413 (1999).
- K. Biradha, C. Seward, and M. J. Zaworotko, *Angew. Chem., Int. Ed. Engl.* **38**, 492 (1999).
- M. J. Zaworotko, *Chem. Rev.* **94**, 283 (1994); S. B. Copp, S. Subramanian, and M. J. Zaworotko, *J. Am. Chem. Soc.* **114**, 8719 (1992); O. R. Evans, Z. Wang, R.-G. Xiong, B. M. Foxman, and W. Lin, *Inorg. Chem.* **38**, 2969 (1999).
- See, for example: O. M. Yaghi, H. Li, and T. L. Groy, *J. Am. Chem. Soc.* **118**, 9096 (1996); S. O. H. Gutschke, M. Molinier, A. K. Powell, E. P. Winpenny, and P. T. Wood, *J. Chem. Soc., Chem. Commun.* 823 (1996); P. Feng, X. Bu, and G. D. Stucky, *Nature* **338**, 735 (1997); D. Hagman, R. P. Hammond, R. Haushalter, and J. Zubieta, *Chem. Mater.* **10**, 2091 (1998); D. J. Chesnut, A. Kusnetzow, R. R. Birge, and J. Zubieta, *Inorg. Chem.* **38**, 2663 (1999).
- (a) J. Y. Lu, B. R. Cabrera, R. J. Wang, and J. Li, *Inorg. Chem.* **37**, 4480 (1998); (b) J. Y. Lu, M. A. Lawandy, J. Li, T. Yuen, and C. L. Lin, *Inorg. Chem.* **38**, 2695 (1999); (c) B. R. Cabrera, R. J. Wang, J. Li, and T. Yuen, in "Solid State Chemistry of Inorganic Materials II" (P. K. Davies, A. J. Jacobson, C. C. Torardi, and T. A. Vanderah, Eds.), Vol. 453, pp. 493–498. MRS, Pittsburgh, 1999; (d) J. Y. Lu, B. R. Cabrera, R. J. Wang, and J. Li, *Inorg. Chem.* **38**, 4608 (1999); (e) M. A. Lawandy, X. Y. Huang, J. Y. Lu, J. Li, T. Yuen, and C. L. Lin, *Inorg. Chem.* **38**, 5410 (1999); (f) L. Pan, X.-Y. Huang, J. Li, Y.-G. Wu, and N.-W. Zheng, *Angew. Chem.* **39**, 527 (2000); (g) L. Pan, X.-Y. Huang, and J. Li, *Inorg. Chem.*, submitted.
- C. B. Aakeroy and A. M. Beatty, *J. Chem. Soc., Chem. Commun.* 1067 (1998); V. A. Russell, C. C. Evans, W. Li, and M. D. Ward, *Science* **276**, 575 (1997).
- R. G. Pearson, *J. Am. Chem. Soc.* **85**, 3533 (1963); G. L. Miessler, and D. A. Tarr, in "Inorganic Chemistry," pp. 197–202. Prentice-Hall, Englewood Cliffs, NJ, 1991.
- G. Kopfmann and R. Hubber, *Acta Crystallogr., A* **24**, 348 (1968).
- A. C. Larson, in "Crystallographic Computing" (F. R. Ahmed, S. R. Hall, and C. P. Huber, Eds.), pp. 291–294. Copenhagen, Munksgaard 1970.
- G. M. Sheldrick, SHELX-97: program for structure refinement, University of Göttingen, Germany, 1997.
- "International Tables for X-ray Crystallography," Vol. C, Tables 4.2.6.8 and 6.1.1.4. Kluwer Academic Publishers, Dordrecht, 1989.
- E. Keller, SCHAKAL 92: a computer program for graphical representation of crystallographic models, University of Freiburg, Germany, 1992.
- G. B. Deacon and R. J. Phillips, *Coord. Chem. Rev.* **33**, 27 (1980).
- M.A. Rollier, S. B. Hendricks, and L. R. Maxwell, *J. Chem. Phys.* **4**, 648 (1936).
- J. K. Shiba and R. Bau, *Inorg. Chem.* **17**, 3484 (1978); K. A. Byriel, L. R. Gahan, C. H. L. Kennard, J. L. Latten, and P. C. Healy, *Aust. J. Chem.* **46**, 713 (1993).
- W. Clegg, I. R. Little, and B. P. Straughan, *Inorg. Chem.* **27**, 1916 (1988); J.-P. Deloume and H. Loiseau, *Acta Crystallogr., B* **30**, 607 (1974).
- L. Pan, X.-Y. Huang, and J. Li, manuscript in preparation.
- B. G. Net, P. Esteban, P. G. Rasmussen, and D. F. Bergstrom, *Inorg. Chem.* **30**, 4771 (1991).
- G. Socrates, "Infrared Characteristic Group Frequencies," 2nd ed. Wiley, London, 1994.